Primary Photoprocesses of Phytochrome. Picosecond Fluorescence Kinetics of Oat and Pea Phytochromes†

Pill-Soon Song* and Bal Ram Singh‡

Molecular Plant Biology Section, School of Biological Sciences, and Department of Chemistry, University of Nebraska, Lincoln, Nebraska 68588

Naoto Tamai, Tomoko Yamazaki, and Iwao Yamazaki

Department of Chemical Process Engineering, Hokkaido University, Sapporo 060, Japan

Satoru Tokutomi and Masaki Furuya§

National Institute for Basic Biology, Okazaki 444, Japan

Received September 28, 1988; Revised Manuscript Received December 22, 1988

ABSTRACT: The primary photoprocesses of etiolated oat and pea phytochromes (Pr forms) are diffusion-modulated by the microscopic viscosity within the chromophore pocket. The chromophore pocket is preferentially accessible to glycerol but not to Ficoll. Glycerol preferentially retarded the rate (rate constant ca. $1-2 \times 10^{10}\ s^{-1}$) of the initial reaction from the Q_y excited state of phytochrome, whereas it increased the long fluorescence lifetime (nanosecond) component that can be attributed to either an emitting intermediate or to modified/conformationally heterogeneous phytochrome populations. The picosecond time-resolved fluorescence spectra of different phytochrome preparations (i.e., full-length vs 6/10-kDa NH_2-terminus truncated forms of phytochromes from monocot and dicot plants) revealed no significant differences. The spectra in the picosecond time scale showed no spectral shifts, but at longer time scales of up to ~1.90 ns, significant blue spectral shifts were observed. The shifts were more in the truncated than in the full-length pea phytochrome. Comparison of the fluorescence decay data and the picosecond time-resolved fluorescence spectra suggests differences in conformational flexibility/heterogeneity among the preparations of the monocot vs dicot phytochromes and the full-length native vs the amino terminus truncated phytochromes.

Phytochrome is the primary photoreceptor chromoprotein that mediates a variety of morphogenic and developmental responses of plants to light, including the regulation of light-responsive gene expression. Modulation of these photoresponses is achieved by the photoreversible transformation of the phytochrome molecule between its inactive (Pr) and active (Pfr) forms, according to the photochromic scheme [for reviews, see Lagarias (1985), Furuya (1987) and reviews cited therein, and Song (1988)]

$$\mathrm{Pr} \underset{\text{730-nm light}}{\overset{\text{660-nm light}}{\rightleftharpoons}} \mathrm{Pfr} \rightarrow \text{biological action}$$

To have a high quantum efficiency, photobiological receptors such as rhodopsin, bacteriorhodopsin, and the reaction center chlorophylls utilize an ultrafast primary reaction in their excited singlet state, in competition with other energy-wasting relaxation processes such as internal conversion, intersystem crossing, and fluorescence emission. Phytochrome is no exception, as its primary photoreaction takes place on a picosecond time scale (Wendler et al., 1984; Holzwarth et al., 1984; Song et al., 1986; Brock et al., 1987), with a quantum yield of 0.5 or greater (Heihoff et al., 1987).

To probe the nature of the primary photoprocesses of phytochrome, we have studied the fluorescence properties of the chromoprotein (Song et al., 1973, 1975, 1979; Sarkar & Song, 1981; Moon et al., 1985). On the basis of an analogy to free base porphyrins and the enhancing effect of deuterium oxide on the fluorescence intensity of phytochrome, it was postulated that proton transfer plays an important role in the primary photoprocess of phytochrome (Song et al., 1979, 1981b). It has also been suggested that proton transfer takes place during the photoconversion process prior to the formation of a spectrally bleached intermediate (Tokutomi et al., 1988). A recent NMR study has shown that photoisomerization occurs during the phototransformation of phytochrome from its Pr to its Pfr form (Ruediger et al., 1983). The isomerization adequately accounts for the primary photoprocess of phytochrome. Furthermore, picosecond decay kinetics exhibited very little, if any, solvent deuterium isotope effects (Eilfeld et al., 1986; Brock et al., 1987).

Upon excitation of Pr phytochrome, a significant movement and reorientation of the chromophore occurs as it is phototransformed to the Pfr form (Hahn et al., 1984; Ekelund et al., 1985). In a preliminary study, we have shown that the primary photoprocess of 124-kDa oat phytochrome, possibly involving a chromophore isomerization, is subject to diffusion control (Song et al., 1986), analogous to the photoisomerization of albumin-bound bilirubin that depends on the microscopic viscosity at the binding site (Lamola et al., 1985). In this paper, we elaborate on the nature of the viscosity-dependent primary photoprocesses of phytochrome in terms of macroscopic and microscopic viscous additives, as probed by picosecond fluorescence decays. The nature of the primary photoprocesses has also been elucidated by comparing the mul-

† This work was supported by USPHS, NIH (GM36956 to P.-S.S.) and the Robert A. Welch Foundation (D-182 to P.-S.S.).

* Address correspondence to this author at the Department of Chemistry, University of Nebraska.

‡ Present address: Department of Food Microbiology and Toxicology, University of Wisconsin, Madison, WI 53706.

§ Present address: Frontier Research Program/Riken, Saitama, Japan.

0006-2960/89/0428-3265$01.50/0

ticomponent fluorescence decay kinetics for monocot (oat) and dicot (pea) phytochromes.

Materials and Methods

Phytochrome Isolation and Purification. Undegraded 124-kDa phytochrome was isolated and purified from etiolated oat seedling shoots (*Avena sativa* L. cv. Garry oat, supplied by Stanford Seed Co., Buffalo, NY) according to the method of Chai et al. (1987). The molecular weight and spectroscopic characteristics of the isolated phytochrome preparations were confirmed by the procedures described in Chai et al. (1987). The degraded, amino terminus truncated 118/114-kDa phytochrome from the etiolated oat shoots was isolated and purified according to the method of Song et al. (1981a). The undegraded, 121-kDa phytochrome from the etiolated pea seedlings (*Pisum sativum* cv. Alaska) was isolated, purified, and characterized according to the method of Tokutomi et al. (1986, 1988). The 114-kDa degraded pea phytochrome was extracted and purified from the etiolated pea seedlings according to the procedure of Yamamoto and Furuya (1983) and Tokutomi et al. (1988). The phytochrome preparations used for the picosecond fluorescence decay and time-resolved spectral studies had specific absorbance ratios (SAR = A_{660}/A_{280}) ranging from 0.9 to 1.1. The 121- and 114-kDa phytochromes used had SAR values of 0.65 and 0.98, respectively. No definitive dependence of the decay and spectral properties of the phytochromes on the purity was found outside the experimental errors. The Pr and Pfr forms of phytochrome were prepared in situ by irradiating the sample cuvette with a 738- and 660-nm optical fiber source for 1–2 min, respectively.

Unless stated otherwise, the phytochrome sample solutions having different solvent viscosities were prepared as described previously (Song et al., 1986). Temperature control for the solution was achieved by using a specially built thermoelectric cooler for the cell compartment.

Picosecond Fluorescence Decay Measurements. These measurements were performed by using a synchronously pumped, cavity-dumped dye laser (Spectra Physics 375 and 344S), a mode-locked argon ion laser (Spectra Physics 171-18), and a time-correlated single photon counter, as described elsewhere (Yamazaki et al., 1984, 1985). Optical setup and conditions were essentially identical with those described in our previous paper (Song et al., 1986). The excitation laser power was 0.68 mW/cm^2 at 800 kHz, with the excitation pulse width at 637 nm set at 6–7 ps for most of the runs. Fluorescence detection was achieved by using a microchannel-plate photomultiplier (R1564U; Hamamatsu Corp. Hamamatsu, Japan). To minimize the buildup of the Pfr species of phytochrome resulting from the exposure of the sample solution to the repeated 637-nm excitation laser pulses, the pulse-irradiated area of the solution was actinically irradiated with a far-red light optical fiber source while the solution was magnetically stirred. This conversion source consisted of an Ushio 500-W Xe arc lamp, a water filter, a focal lens (f = 50), a neutral density wedge filter, a 738-nm interference filter (half-maximum bandwidth = 10.5 nm), and a glass optical fiber. The schematics of this optical arrangement have been presented previously (Song et al., 1986). Under these conditions, negligible amounts of Pfr were produced during each data acquisition, which lasts 30–60 s for 2000 counts. Only after an extended period of data acquisition did the excitation laser pulses (beam diameter 1.5 mm) produce appreciable amounts of Pfr in the cuvette, corresponding to ca. 10% conversion from Pr (Song et al., 1986). After the effect of the stirring rate on the measured decay data (lifetimes and their amplitudes) was studied, the magnetic stirrer was set at or above a speed where no significant dependences of the decay parameters on the mixing rate of solution were observed. This stirring-effect study was necessitated by the observation that our previous lifetimes of oat phytochrome in 67% glycerol buffer (Song et al., 1986) were found to be slightly longer than the values obtained in the present study, due to the effect of mixing.

The fluorescence decay curves for various phytochrome sample solutions were analyzed by a least-squares fit (O'Connor & Phillips, 1984) for the multiexponential decays observed (Song et al., 1986). The success of the fit on about 200 decay curves recorded was judged by the reduced χ^2 values (1.0–1.3), the Durbin–Watson parameter (greater than 1.6), and the plots of the weighted residuals and the correlation functions.

Time-Resolved Fluorescence Spectroscopy. By use of the same laser system and optical layout as described above, time-resolved fluorescence spectra of phytochrome were obtained from a series of fluorescence decay curves monitored at different wavelengths of emission. Both the technique and analytical method of the time-resolved fluorescence spectroscopy employed have been described in detail elsewhere (Yamazaki et al., 1984). Briefly, time-resolved fluorescence spectra were obtained from the fluorescence decay curves with a minimum time difference of 0.8 ps by plotting the fluorescence intensities at particular decay times as a function of emission wavelengths.

Results

Fluorescence Decays as a Function of Viscosity. Figure 1 shows the typical fluorescence decay curves obtained for oat phytochrome in various viscosity media; 67% (w/w) glycerol (M_r 92) and 51% sucrose (M_r 342) solutions possess the same macroscopic viscosity at 293 K, whereas a 30% Ficoll (average M_r 400 000) has a viscosity of about 100 cP, which is more than 5 times the viscosity of a 67% glycerol solution (19 cP). According to the least-squares fits, the multiexponential decay curves can be best represented in terms of three components, although the two-component fits may be regarded adequate for describing the decay curves semiquantitatively. Similar results were obtained with 118/114-kDa oat phytochrome. Table I presents the lifetime and amplitude data for oat phytochrome as a function of different medium viscosity. The lifetime of the fastest component increases moderately in 67% glycerol and 51% sucrose, but remains approximately the same in 30% Ficoll and in nonviscous buffers. Furthermore, the amplitudes of the longer components increase in 67% glycerol and 51% sucrose, but not in 30% Ficoll (Table I).

Figure 2 shows the picosecond fluorescence decay curves for 121- and 114-kDa pea phytochromes in different viscosity media. The resolved lifetimes and their amplitudes are presented in Table I. Comparison between the decay data for the oat and pea phytochromes suggests that the overall multicomponent behaviors of the fluorescence decays are essentially the same for both monocot and dicot phytochromes, which were also isolated by mutually different isolation/purification procedures. However, the τ_2 and τ_3 values are significantly greater for pea phytochrome than for oat phytochrome. Furthermore, the effect of 67% glycerol on the τ_1 and τ_2 values appears to be less pronounced for pea phytochrome than for oat phytochrome.

From the data presented in Figures 1 and 2 and Table I, it is clear that the short-lifetime component predominates the fluorescence decays in both oat and pea phytochromes. The amplitude of the longer lifetime component(s) increases sig-

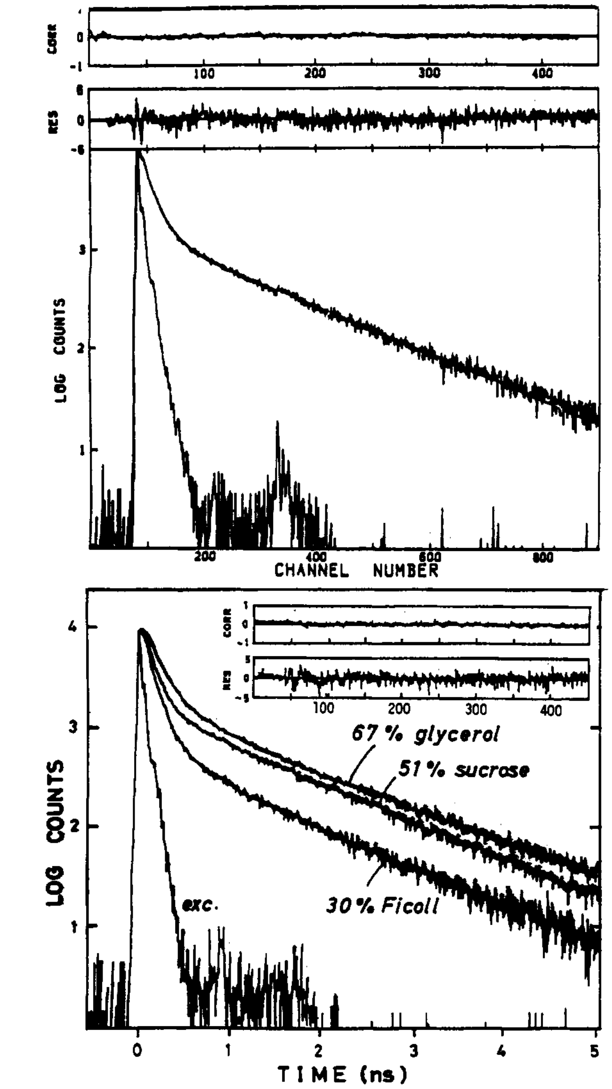

FIGURE 1: Fluorescence decay curves of oat phytochrome (124 kDa) as a function of medium viscosity at 290 K. (Top) Phytochrome in 20 mM potassium phosphate buffer in the absence of any viscous additive. The weighted residuals and the autocorrelation function for the least-squares fit to the decay curve are displayed on the top portion. The abscissa scale is 6.2 ps/channel. (Bottom) Phytochrome in different viscosity media. The excitation wavelength was 637 nm, and the monitoring wavelength was 680 nm. The instrumental response function of the excitation laser pulse (pulse width 40 ps, fwhm) is also shown, along with a typical plot of the autocorrelation function and the weighted residuals (for oat phytochrome in 67% glycerol). Phytochrome was 1.2 μM in 20 mM potassium phosphate buffer, pH 7.8, containing 1 mM EDTA and 67% glycerol (or 51% sucrose or 30% Ficoll v/v). The specific absorbance ratios (SAR = A_{660}/A_{280}) of the phytochromes used were in the range 0.90–1.1.

nificantly in 67% glycerol and moderately in 51% sucrose, whereas it remains virtually identical for the phytochrome solutions in 30% Ficoll and in aqueous buffer without any viscous additive.

Time-Resolved Fluorescence Spectra. Figure 3 shows the time-resolved fluorescence spectra of oat (124 kDa) and pea (121 and 114 kDa) phytochromes in 67% glycerol. The sample solution was simultaneously irradiated with a continuous actinic light of 738-nm wavelength. It can be seen that the time-resolved fluorescence spectrum with a peak at ca. 685 nm remains virtually constant over the time domain covered, except for an apparent blue shift of ca. 10 nm for the emission peak at times greater than 500 ps after the excitation pulse. The time-resolved fluorescence spectra of pea phytochromes (114 and 121 kDa) in 67% glycerol are also shown in Figure 3. For both the 114- and 121-kDa pea phytochromes, the emission maximum changes to the blue at 1 ns longer after an excitation pulse. This blue shift appears to be somewhat more prominent with the pea phytochromes, especially the 114-kDa species, than with oat phytochrome.

Table I: Fluorescence Lifetimes and Their Percent Amplitudes for Oat and Pea Phytochromes as a Function of Emission Wavelength and Viscosity[a]

sample[b]	emission (nm)	lifetimes (ps) τ_1	τ_2	τ_3	% amplitude τ_1	τ_2	τ_3
124-kDa oat, KPB	670	30.8	136.6	1167.1	86.2	12.6	1.2
	680	39.6	167.0	1145.0	90.2	8.8	1.0
	690	38.6	144.2	1071.0	88.4	10.8	0.8
	700	42.4	158.9	1063.0	90.9	8.5	0.5
av		37.9	151.7	1112.0	88.9	10.2	0.9
124-kDa oat, 67% glycerol	660	61.1	319.9	1269.0	70.3	17.5	12.2
	670	50.8	245.8	1211.0	75.1	15.8	9.1
	680	50.8	238.5	1187.0	77.7	15.6	6.7
	690	49.9	206.7	1146.0	79.0	15.3	5.6
	700	62.9	287.0	1204.0	78.6	14.0	7.4
av		53.6	244.5	1187.0	77.6	15.6	8.2
124-kDa oat, 51% sucrose	670	38.5	204.4	1145.2	81.9	11.2	6.9
	680	41.1	176.8	1133.0	83.9	10.5	5.6
	690	48.4	219.7	1100.1	86.8	8.1	5.1
	700	46.5	204.7	1091.6	84.8	9.6	5.6
av		43.6	201.4	1117.5	84.4	9.9	5.8
124-kDa oat, 30% Ficoll	670	36.9	164.2	1093.6	82.5	14.0	3.5
	680	38.8	175.1	1013.0	86.5	11.1	2.4
	690	38.4	138.7	948.8	85.3	12.9	1.9
	700	41.0	154.1	961.1	87.4	10.7	2.0
av		38.8	158.0	1004.0	85.4	12.2	2.5
121-kDa pea, HEPES	660	39.6	273.5	1694.2	90.3	8.4	1.3
	670	37.8	244.1	1393.0	92.0	7.2	0.8
	680	39.1	233.6	1268.0	93.5	6.0	0.5
	690	39.7	233.3	1217.6	93.8	5.7	0.5
	700	39.0	215.3	1082.6	93.9	5.6	0.5
av		39.0	239.9	1331.0	92.7	5.5	0.7
121-kDa pea, KPB	670	47.3	240.0	1454.0	86.5	11.7	1.8
	680	47.5	220.9	1300.0	89.2	9.6	1.2
	690	46.5	212.7	1284.0	89.9	9.2	0.9
	700	50.2	240.7	1611.9	91.2	8.1	0.7
av		47.9	228.6	1412.0	89.2	9.7	1.1
121-kDa pea, 67% glycerol	660	43.5	255.7	1313.4	80.2	15.8	4.0
	670	51.3	257.0	1248.3	80.2	16.2	3.6
	680	54.7	232.5	1203.0	82.0	15.0	3.0
	690	57.2	265.6	1170.6	83.4	13.7	2.9
	700	58.7	282.3	1198.9	85.6	11.8	2.6
av		53.1	258.6	1227.0	82.3	14.5	3.2
114-kDa pea, HEPES	660	28.6	219.8	2403.9	93.9	4.9	1.2
	670	33.3	255.6	2058.0	96.3	3.0	0.7
	680	34.3	261.0	1953.0	97.7	2.0	0.3
	690	34.9	252.8	1857.0	97.9	1.9	0.2
	700	34.8	231.8	1498.7	97.4	2.4	0.2
	710	36.8	243.1	1500.2	97.5	2.3	0.2
av		33.8	244.0	1878.0	96.8	2.8	0.4
114-kDa pea, 40% glycerol	660	32.0	207.0	1902.3	91.0	7.6	1.4
	670	36.4	223.6	1591.6	93.7	5.5	0.8
	680	37.5	231.0	1436.0	95.1	4.4	0.5
	690	41.4	237.2	1365.5	95.6	4.0	0.4
	700	40.0	229.9	1287.2	95.6	4.0	0.4
	710	39.4	236.4	1471.4	95.8	3.9	0.3
av		37.8	227.5	1509.0	94.5	4.9	0.8
114-kDa pea, 16% glycerol	660	38.9	236.3	1702.0	87.9	9.9	2.2
	670	41.3	241.3	1484.9	90.3	8.2	1.5
	680	42.3	231.7	1311.0	91.1	7.8	1.1
	690	43.7	220.4	1220.9	91.0	7.9	1.1
	700	43.3	216.0	1225.9	90.9	8.1	1.0
av		41.9	229.1	1389.0	90.2	8.4	1.4

[a] See Materials and Methods for measurement details and experimental conditions. [b] KPB, potassium phosphate buffer, pH 7.8. HEPES, HEPES buffer, pH 7.8.

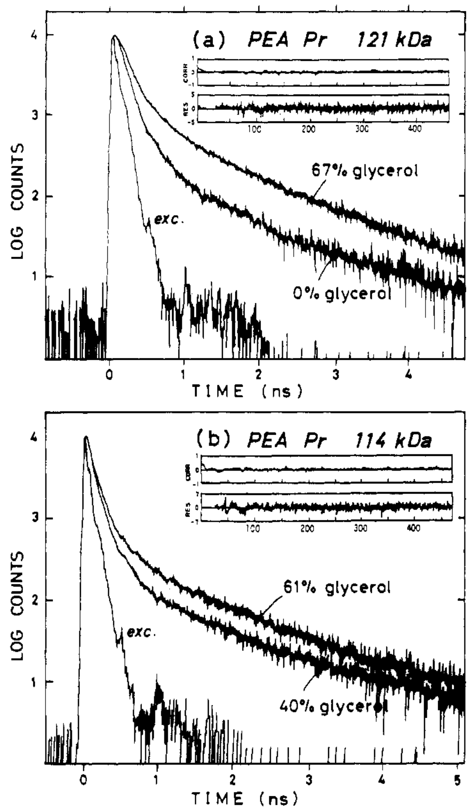

FIGURE 2: Fluorescence decay curves of pea phytochrome as a function of viscosity at 286 K. (a) 121-kDa phytochrome (SAR 0.65) and (b) 114-kDa phytochrome (SAR 0.98) in 25 mM HEPES buffer, pH 7.8, containing 1 mM EDTA. Other measurement conditions are identical with those described in the caption for Figure 1, except for a larger pulse width, 60 ps (fwhm). The autocorrelation functions and the weighted residuals for Pr in 67% glycerol (top) and Pr in 61% glycerol (bottom) are also shown. The abscissa scale is 6.2 ps/channel.

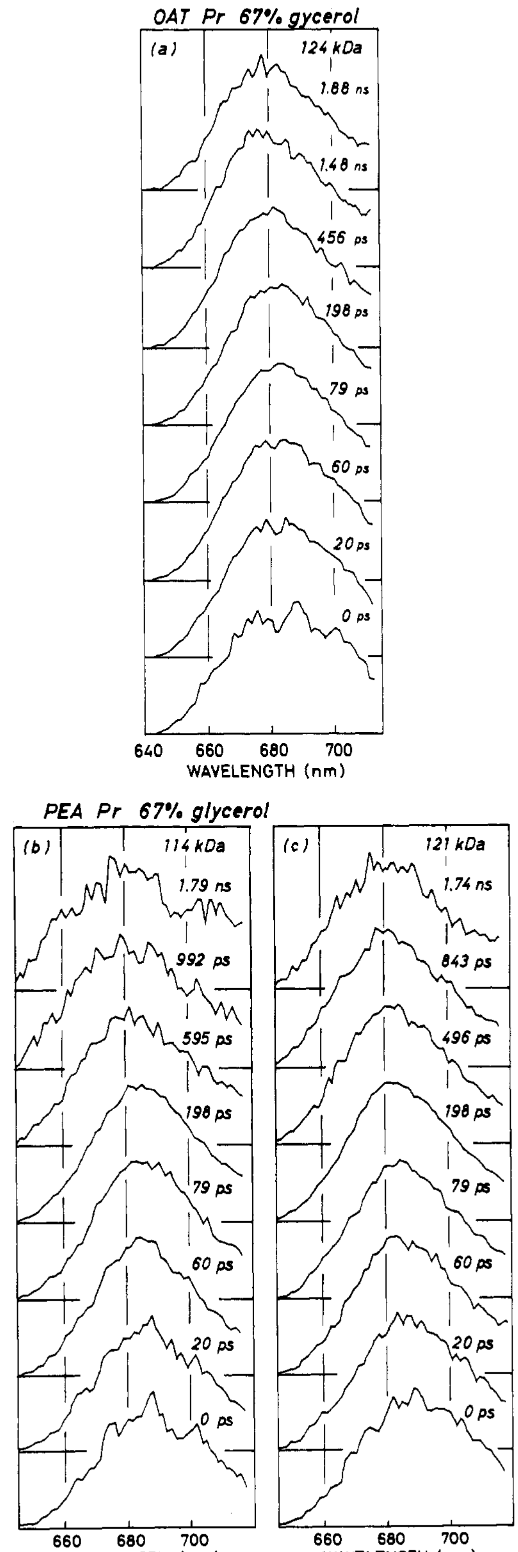

FIGURE 3: Time-resolved fluorescence spectra of 124-kDa oat (a) and 114-kDa (b) and 121-kDa pea (c) phytochromes in 67% glycerol. The excitation wavelength was 637 nm. The time zero corresponds to the time at which the excitation pulse reaches a maximum intensity. The sample preparation and conditions are the same as in Figures 1 and 2.

The time-resolved fluorescence spectra of phytochromes within 500 ps were found to be independent of medium viscosity, i.e., 67% glycerol (data not shown). However, a long-lived species with an emission maximum at ca. 660 nm or shorter was determined from the time-resolved spectra of 114-kDa pea phytochrome in phosphate buffer without glycerol at times longer than 1 ns after an excitation pulse, independent of far-red actinic irradiation and magnetic stirring (Figure 4). The long-lifetime species was resolvable from the time-resolved fluorescence spectra independent of the mixing and the 738-nm actinic irradiation of the sample solution. However, the species emitting at ca. 660 nm is not seen in a 67% glycerol solution (Figure 3), suggesting that the formation of this species is retarded in the viscous medium.

The time-resolved fluorescence spectra of phytochrome in 30% Ficoll were similar to those in 0% and 67% glycerol. Figure 5 shows a typical set of the emission spectra of 124-kDa oat phytochrome in 30% Ficoll.

To follow a fast movement of the chromophore of phytochrome in its excited state, fluorescence anisotropy decays of 124-kDa oat phytochrome in 67% glycerol were measured (Figure 6). It can be seen that the anisotropy declines initially by ca. 0.04.

Discussion

To interpret the viscosity dependences of the fluorescence decay data on phytochrome, the following points from the previous section are highlighted and will be discussed.

(1) The fluorescence decay of phytochrome is multiexponential; three exponential components can best account for the complex decay curves shown in Figures 1 and 2. The short component is the major contributor to the fluorescence decays. This observation confirms the previous results with oat (Holzwarth et al., 1984; Wendler et al., 1984; Song et al., 1986) and rye (Lippitsch et al., 1988) phytochromes.

(2) The short-component lifetime and the long-component amplitudes increase in 67% glycerol, compared to those in

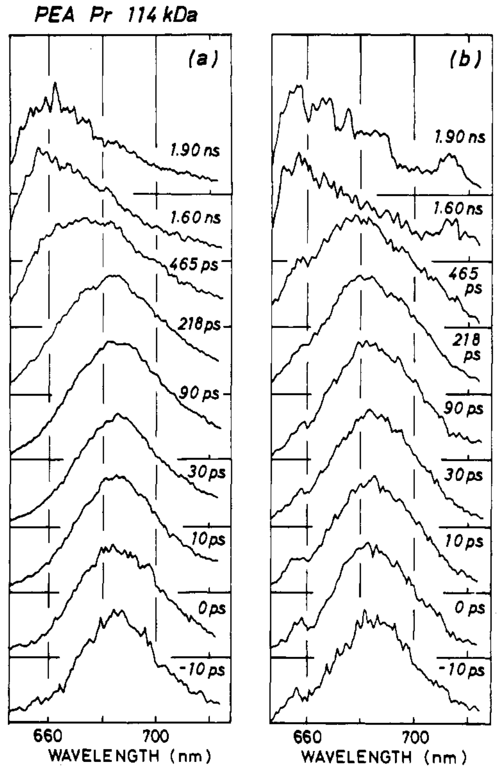

FIGURE 4: Time-resolved fluorescence spectra of 114-kDa pea phytochrome in 100 mM potassium phosphate buffer, pH 7.8, containing 1 mM EDTA at 290 K. Experimental conditions are identical with those in Figure 3. (a) Without far-red actinic irradiation and magnetic stirring; (b) with far-red actinic irradiation and magnetic stirring (see Materials and Methods).

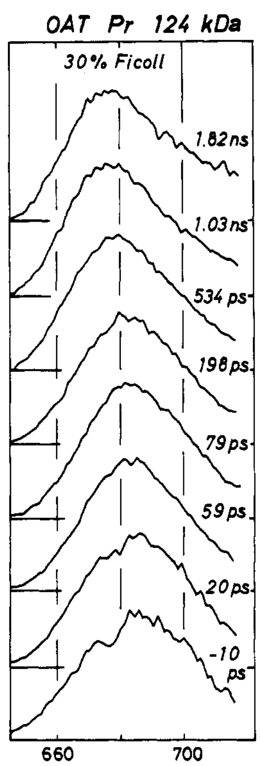

FIGURE 5: Time-resolved fluorescence spectra of 124-kDa oat phytochrome in 30% Ficoll. See Figure 3 for measurement conditions.

nonviscous buffers, but show almost no increase in 30% Ficoll. In 51% sucrose, these parameters take on intermediate values between those in 67% glycerol and 30% Ficoll. The lifetime of the 1.1-ns component is not affected by medium viscosity, however (Table I).

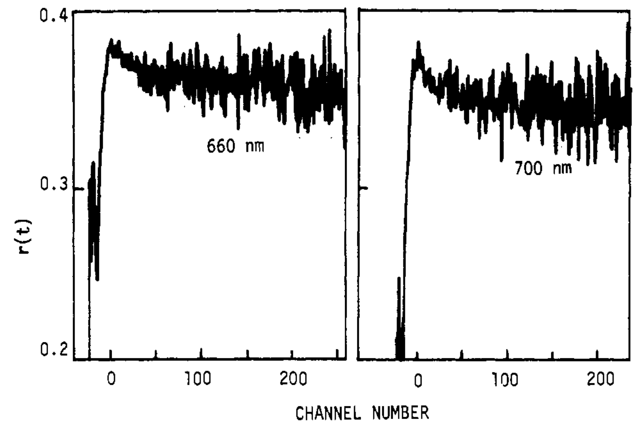

FIGURE 6: Fluorescence anisotropy decays ($r(t)$) of 124-kDa oat phytochrome (1.2 μM) in 67% glycerol in 20 mM potassium phosphate buffer, pH 7.8, containing 1 mM EDTA at 290 K. The excitation wavelength was 637 nm; the monitoring wavelength was 660 (left) and 700 nm (right). The abscissa scale is 6.2 ps/channel. For fluorescence anisotropy measurements, an analyzing polarizer was placed between the sample compartment and a depolarizer placed in front of the photomultiplier. The depolarizer was used to remove any polarization-sensitive bias of the photomultiplier.

(3) Qualitatively, the monocot and dicot phytochromes exhibit similar decay characteristics in terms of multicomponent lifetimes and their relative amplitudes. However, the two longer component lifetimes of the latter tend to be reproducibly greater than the corresponding values of the former (Table I).

(4) Within a few hundred picosecond range, there is no significant time resolution of the fluorescence emission spectra of both oat and pea phytochromes. A significant blue shift of the emission maxima occurs in the nanosecond region, which appears to be slightly dependent on the medium viscosity (the least shift is in 67% glycerol) but strongly dependent on the integrity (M_r) of pea phytochrome (Figure 4).

There are several interpretations for the three-component decays of phytochromes. We will discuss here two of the most likely models. Model I is to assume that only the shortest, predominant lifetime component reflects the radiative and radiationless relaxation processes of the Q_y excited state of phytochrome. The two longer components represent the fluorescence decays of "denatured" or "modified" phytochromes, consistent with Holzwarth et al. (1984). Thus, the primary photoprocesses of phytochrome can be represented as

$$\mathrm{Pr} + h\nu \rightarrow \mathrm{Pr}^* \quad (Q_y \text{ excited state})$$

$$\mathrm{Pr}^* \xrightarrow{k_{rx}} \mathrm{Pr}' \quad (\phi_{rx} = 0.5;\ \text{Heihoff et al., 1987})$$

$$\mathrm{Pr}^* \xrightarrow{k_{rl}} \mathrm{Pr} + \text{heat} \quad (\phi_{rl} = 0.5;\ \text{Heihoff et al., 1987})$$

$$\mathrm{Pr}^* \xrightarrow{k_f} \mathrm{Pr} + \text{fluorescence} \quad (\phi_f = 0.003;\ \text{Holzwarth et al., 1984})$$

where ϕ_{rx}, ϕ_{rl}, and ϕ_f are quantum yields for the primary reaction (k_{rx}), radiationless heat dissipation (k_{rl}), and fluorescence emission (k_f), respectively.

Using the relation

$$k_{rx} = \phi_{rx}/\tau_f$$

where τ_f is the measured fluorescence lifetime (38 ± 8 ps; Table I) at ambient temperature, one obtains $k_{rx} = 1.3 \times 10^{10}$ s^{-1}, which is comparable to a diffusion-controlled rate constant in an aqueous medium. The same value can be calculated for

Table II: Fluorescence Lifetimes, Percent Amplitudes, and Rate Constants (k_1 and k_{-1}) for Oat and Pea Phytochromes in Different Viscous Media, Calculated from the Two-Component Lifetime Fits to the Observed Fluorescence Decay Curves[a]

			lifetimes (ps)		rate constants (s^{-1})	
Pr[b]	medium[c]	η/η_0[d]	τ_1 (%)	τ_2 (%)	$k_1 \times 10^{-10}$	$k_{-1} \times 10^{-8}$
124-kDa oat	KPB	1.0	36.2 (98.8)	1102 (1.2)	2.7	3.3
	67% GOH	19.0	45.6 (93.1)	1157 (6.9)	2.0	15.1
	51% SOH	19.0	43.0 (93.3)	1147 (6.7)	2.2	15.6
	30% FCL	100.0	38.8 (97.4)	1073 (2.6)	2.5	6.7
118-kDa oat	KPB	1.0	45.1 (98.8)	1219 (1.2)	2.2	2.8
121-kDa pea	KPB	1.0	46.3 (98.8)	1279 (1.2)	2.1	2.6
	HEPES	1.0	34.1 (99.5)	1252 (0.5)	2.9	1.6
	67% GOH	19.0	53.3 (96.5)	1206 (3.5)	1.8	6.6
114-kDa pea	HEPES	1.0	36.2 (99.7)	1956 (0.3)	2.8	0.8
	40% GOH	3.1	35.1 (99.6)	1434 (0.4)	2.8	1.2
	61% GOH	17.3	42.3 (98.8)	1308 (1.2)	2.3	2.9

[a] See text for details. [b] Red-absorbing form of phytochrome (Pr). [c] KPB, potassium phosphate buffer; GOH, glycerol; SOH, sucrose; HEPES, HEPES buffer; FCL, Ficoll. [d] Relative viscosities.

121-kDa pea phytochrome in HEPES buffer. The k_{rx} value decreases with viscous additives (1.1×10^{10} s^{-1} in 51% sucrose and 9.2×10^9 s^{-1} in 67% glycerol), but not with 30% Ficoll (1.3×10^{10} s^{-1}).

Model II (Song et al., 1986) assumes that the multiexponential decays shown in Figures 1 and 2 can be adequately represented by two exponentials. Under these assumptions, the three-component fit is replaced by the two-component fit in terms of two lifetimes, 30–50 ps and 1–2 ns, without significantly sacrificing the quality of least-squares fits [cf. Song et al. (1986)]. Table II shows a set of such fits that were performed without any preselected constraints as to which of the two longer lifetime components (second and third components shown in Table I) can be neglected. The following scheme qualitatively accounts for the two-component model

$$\mathrm{Pr} + h\nu \rightarrow \mathrm{Pr}^* \qquad (\mathrm{Q_y}\text{ excited state})$$

$$\mathrm{Pr}^* \underset{k_{-1}}{\overset{k_1}{\rightleftharpoons}} \mathrm{Pr}' \qquad (\text{reversible primary reaction})$$

$$\mathrm{Pr}^* \xrightarrow{k_f} \mathrm{Pr} + \text{fluorescence}$$

$$\mathrm{Pr}' \xrightarrow{k_2} \text{lumi-R(?)}$$

where k_1 corresponds to k_{rx} in model I. Model II leads to the expressions (Song & Yamazaki, 1987)

$$k_1 = \tau_1^{-1}(1 + (A_2/A_1))$$

$$k_{-1} = k_1(A_2/A_1)$$

where $\tau_1 = (k_1 + k_{-1})^{-1}$ and $A_{1,2}$ represent the relative amplitudes of the two lifetime components. Table II presents the calculated values for k's. The calculated k_1 values are similar in magnitude to the k_{rx} values estimated from the scheme for model I. It should be noted that these values are reduced by 67% glycerol and 51% sucrose, compared to the data in nonviscous buffers, but are unaffected by 30% Ficoll. Other alternative models may be suggested, but it appears that the rate constant for the primary reaction is not expected to vary greatly, since the short-lifetime component predominates the fluorescence decay curves of oat and pea phytochromes in different media.

The nature of the primary reaction in the above models is not known at present. An initial intermediate arising from the primary reaction is either lumi-R [or I_{700}; Heihoff et al., 1987; see review by Song (1988)] or prelumi-R, which may be formed prior to lumi-R (Song et al., 1981, 1986; Lippitsch et al., 1988). A recent study based on both picosecond absorption and fluorescence of rye phytochrome assigns 40 ps to the formation of prelumi-R, followed by the formation of lumi-R with a time constant of 60 ps (Lippitsch et al., 1988). Since photoisomerization about a C=C bond in a conjugated molecule can take place at picosecond and femtosecond time scales (e.g., cis-trans isomerization in bacteriorhodopsin taking place in ca. 0.5 ps; Mathies et al., 1988), the proposed *E-Z* photoisomerization of the 15 C=C bond of the tetrapyrrole chromophore of phytochrome (Ruediger et al., 1983) must similarly occur from the Q_y excited state of the phytochrome molecule. Since the Pr chromophore of phytochrome is buried in a hydrophobic binding pocket (Hahn et al., 1984; Song & Yamazaki, 1987), it is reasonable that the movement/isomerization of the chromophore therein is apparently sensitive to glycerol but not to Ficoll, as the pocket would be most readily accessible to the small glycerol molecule but not to the larger Ficoll molecule. Sucrose with its M_r greater than that of glycerol but considerably smaller than that of Ficoll also moderately retards the primary reaction. The similar dependence of the amplitude of the nanosecond component (Table II) on these viscous additives can be satisfactorily explained in terms of model II discussed above, although the observation can also be reconciled with model I or its variants.

Comparison of the fluorescence decay data and time-resolved fluorescence spectra between the monocot and dicot phytochromes (Table I and Figures 1–3) reveals some subtle differences. In contrast to oat phytochrome, the fluorescence decay curves for 118/114-kDa oat and 114-kDa pea phytochromes yield a significantly smaller value for k_{-1} than for the undegraded full-length phytochrome preparations (Table II). This is attributable to a markedly smaller contribution of the nanosecond component to the fluorescence decay curves and to the relatively larger time-resolved spectral shift that is seen with the degraded pea phytochrome (Figure 3) than is seen with the other preparations. From Table II, k_1 for the amino terminus truncated phytochromes also depends moderately on the medium viscosity, whereas k_{-1} increases significantly and preferentially with increasing concentration of the smallest viscous molecule, glycerol, as in the case of the full-length native phytochromes. There are also noticeable differences in the k_1 and k_{-1} values between oat and pea phytochromes (Table II). The differential glycerol dependences of these rates may arise from a restricted conformational flexibility of the chromophore and the surrounding residues in the excited state and its primary intermediate.

Since phytochrome exists as a dimer (248 kDa) in solution (Jones & Quail, 1986), its Brownian rotation is negligible in 67% glycerol at picosecond time scales. However, the chromophore in its apoprotein pocket may exhibit an orientational tumbling during the relaxation processes (k_1 and k_{-1}), according to model II. This is borne out, as the fluorescence anisotropy decays rapidly by about 0.04 during the first 500-ps range (Figure 6).

Alternatively, according to model I, the lower k_{-1} values for the amino terminus truncated phytochromes exhibit a substantially lower contribution from the nanosecond component to the overall fluorescence decays, as the long-lifetime contaminant(s) is minimized in these degraded phytochrome preparations. The blue-shifted emission at times longer than 1 ns after the pulse excitation (Figures 3 and 4) can then be assigned to such a contaminant or heterogeneity in the phytochrome populations, according model I. However, it is important to note that the significant increase in the amplitude of the nanosecond component in 67% glycerol is not accompanied by a blue shift of the time-resolved emission spectra (Figures 3–5). This implies that the nanosecond component cannot be entirely attributed to a contaminant emission.

The fluorescence lifetimes also depend on the buffers used, i.e., phosphate vs HEPES (Table I). Lagarias and Mercurio (1985) found a significant effect of different buffers on the gel filtration profiles of phytochrome, suggesting gross conformational differences in the protein in different buffers. However, we have no evidence for gross conformational perturbations of the phytochrome molecule by glycerol, sucrose, and Ficoll. Thus, the differences in lifetimes and their amplitudes in varying viscosity media are explicable in terms of a microenvironmental conformational flexibility, which is diffusion-modulated by the microscopic viscosity within the chromophore pocket or elsewhere in the apoprotein (accessible preferentially to glycerol).

Finally, we note that an attempt to study the primary photoprocesses of the Pfr form of phytochrome by using a new near-IR-sensitive S-1 photomultiplier tube (Hamamatsu Model 1564U-05) operated at −30 °C was not successful, as fluorescence emission from the Pfr form was undetectable.

Acknowledgments

P.-S.S. thanks the Institute for Molecular Science (Director Professor S. Nagakura) for providing him with a visiting professorship in 1987 that made the collaborative study possible. We thank Debbie Sommer and William Parker for reading the first draft.

References

Brock, H., Ruzsicska, B. P., Arai, T., Schlamann, W., Holzwarth, A. R., Braslavsky, S. E., & Schaffner, K. (1987) *Biochemistry 26*, 1412–1417.

Chai, Y. G., Singh, B. R., Song, P. S., Lee, J., & Robinson, G. W. (1987a) *Anal. Biochem. 163*, 322–330.

Chai, Y. G., Song, P. S., Cordonnier, M. M., & Pratt, L. H. (1987b) *Biochemistry 26*, 4947–4952.

Eilfeld, P., Eilfeld, P. E., & Ruediger, W. (1986) *Photochem. Photobiol. 44*, 761–769.

Ekelund, N. G. A., Sundqvist, C., Quail, P. H., & Vierstra, R. D. (1985) *Photochem. Photobiol. 41*, 221–223.

Furuya, M. (Ed.) (1987) *Phytochrome and Photoregulation in Plants*, Academic Press, Tokyo.

Hahn, T. R., Song, P. S., Quail, P. H., & Vierstra, R. D. (1984) *Plant Physiol. 74*, 755–758.

Heihoff, K., Braslavsky, S. E., & Schaffner, K. (1987) *Biochemistry 26*, 1422–1427.

Holzwarth, A. R., Wendler, J., Ruzsicska, B. P., Braslavsky, S. E., & Schaffner, K. (1984) *Biochim. Biophys. Acta 791*, 265–273.

Jones, A. M., & Quail, P. H. (1986) *Biochemistry 25*, 2987–2995.

Lagarias, J. C. (1985) *Photochem. Photobiol. 42*, 811–820.

Lagarias, J. C., & Mercurio, F. M. (1985) *J. Biol. Chem. 260*, 2415–2423.

Lamola, A. A. (1985) in *Optical Properties and Structure of Tetrapyrroles* (Blauer, G., & Sund, H., Eds.) pp 311–330, de Gruyter, Berlin.

Lippitsch, M. E., Riegler, H., Aussenegg, R. R., Hermann, G., & Muller, E. (1988) *Biochem. Physiol. Pflanz. 183*, 1–6.

Mathies, R. A., Brito Cruz, C. H., Pollard, W. T., & Shank, C. V. (1988) *Science 240*, 777–779.

Moon, D. K., Jeen, G. S., & Song, P. S. (1985) *Photochem. Photobiol. 41*, 633–648.

O'Connor, D. V., & Phillips, D. (1984) *Time-Correlated Single Photon Counting*, pp 171–193, Academic Press, New York.

Ruediger, W., Thuemmler, F., Cmiel, E., & Schneider, S. (1983) *Proc. Natl. Acad. Sci. U.S.A. 80*, 6244–6248.

Sarkar, H. K., & Song, P. S. (1981) *Biochemistry 20*, 4315–4320.

Song, P. S. (1988) *J. Photochem. Photobiol., B 2*, 43–57.

Song, P. S., & Yamazaki, I. (1987) in *Phytochrome and Photoregulation in Plants* (Furuya, M., Ed.) pp 139–156, Academic Press, Tokyo.

Song, P. S., Chae, Q., Lightner, D. A., Briggs, W. R., & Hopkins, D. (1973) *J. Am. Chem. Soc. 95*, 7892–7893.

Song, P. S., Chae, Q., & Briggs, W. R. (1975) *Photochem. Photobiol. 22*, 74–75.

Song, P. S., Chae, Q., & Gardner, J. G. (1979) *Biochim. Biophys. Acta 576*, 479–495.

Song, P. S., Kim, I. S., & Hahn, T. R. (1981a) *Anal. Biochem. 117*, 32–39.

Song, P. S., Sarkar, H. K., Kim, I. S., & Poff, K. L. (1981b) *Biochim. Biophys. Acta 635*, 369–382.

Song, P. S., Tamai, N., & Yamazaki, I. (1986) *Biophys. J. 49*, 645–649.

Tokutomi, S., Inoue, Y., Sato, N., Yamamoto, K. T., & Furuya, M. (1986) *Plant Cell Physiol. 27*, 765–773.

Tokutomi, S., Yamamoto, K. T., & Furuya, M. (1988) *Photochem. Photobiol. 47*, 439–445.

Wendler, J., Holzwarth, A. R., Braslavsky, S. E., & Schaffner, K. (1984) *Biochim. Biophys. Acta 786*, 213–221.

Yamamoto, K. T., & Furuya, M. (1983) *Plant Cell Physiol. 24*, 713–718.

Yamazaki, I., Mimuro, M., Murao, T., Yamazaki, T., Yoshihara, K., & Fujita, Y. (1984) *Photochem. Photobiol. 39*, 233–240.

Yamazaki, I., Tamai, N., Kume, H., Tsuchiya, H., & Oba, K. (1985) *Rev. Sci. Instrum. 56*, 1187–1193.